



Molecular Crystals and Liquid Crystals Science and Technology. Section A. Molecular Crystals and Liquid Crystals

Publication details, including instructions for authors and
subscription information:

<http://www.tandfonline.com/loi/gmcl19>

Overview of 10K Class Organic Superconductors κ -(BEDT-TTF)₂X (X = Cu (NCS)₂, Cu(CN)[N(CN)₂], Cu[N(CN)₂]X' (X' = Cl, Br) and a Search for Superconductivity in Alkali Doped C₆₀ Complexes

G. Saito^a, A. Otsuka^a & A. A. Zakhidov^b

^a Dep. of Chem., Grad. School of Sci., Kyoto Univ., Kyoto,
606-01, Japan

^b Institute for Molecular Science, Myodaiji, Okazaki, 444, Japan
Version of record first published: 24 Sep 2006.

To cite this article: G. Saito, A. Otsuka & A. A. Zakhidov (1996): Overview of 10K Class Organic Superconductors κ -(BEDT-TTF)₂X (X = Cu (NCS)₂, Cu(CN)[N(CN)₂], Cu[N(CN)₂]X' (X' = Cl, Br) and a Search for Superconductivity in Alkali Doped C₆₀ Complexes, Molecular Crystals and Liquid Crystals Science and Technology. Section A. Molecular Crystals and Liquid Crystals, 284:1, 3-14

To link to this article: <http://dx.doi.org/10.1080/10587259608037906>

PLEASE SCROLL DOWN FOR ARTICLE

Full terms and conditions of use: <http://www.tandfonline.com/page/terms-and-conditions>

This article may be used for research, teaching, and private study purposes. Any substantial or systematic reproduction, redistribution, reselling, loan, sub-licensing, systematic supply, or distribution in any form to anyone is expressly forbidden.

The publisher does not give any warranty express or implied or make any representation that the contents will be complete or accurate or up to date. The accuracy of any instructions, formulae, and drug doses should be independently verified with primary sources. The publisher shall not be liable for any loss, actions,

claims, proceedings, demand, or costs or damages whatsoever or howsoever caused arising directly or indirectly in connection with or arising out of the use of this material.

OVERVIEW OF 10K CLASS ORGANIC SUPERCONDUCTORS κ -(BEDT-TTF)₂X (X=Cu(NCS)₂, Cu(CN)[N(CN)₂], Cu[N(CN)₂]X' (X'=Cl, Br) AND A SEARCH FOR SUPERCONDUCTIVITY IN ALKALI DOPED C₆₀ COMPLEXES

G. Saito, A. Otsuka, A. A. Zakhidov*,
Dep. of Chem., Grad. School of Sci., Kyoto Univ., Kyoto
606-01, Japan *Institute for Molecular Science,
Myodaiji, Okazaki 444, Japan

Abstract The curious structural and physical properties of the 10K class BEDT-TTF superconductors having polymerized anions and the superconductivity of the alkali doped C₆₀ organic CT complexes are described.

INTRODUCTION

For oxide superconductors, the superconductivity (SC) is realized by carrier doping (or band filling control) into the Mott insulators. As for the organic materials several band filling methods have been applied such as, gas phase doping, electrochemical doping, substitution of the component molecules having different charge, ionization potential or electron affinity, etc. So far, however, only one example has been known which realizes SC after carrier doping, without changing the original crystal structure, into a Mott insulator at ambient pressure, namely κ -(BEDT-TTF)Cu₂(CN)₃.¹ Not so wide bandwidth (W=0.5-1eV) of BEDT-TTF(ET) conductors makes the screening of electrons not effective leading an enhancement of the electron correlation. Since the W values of them are comparable or less than the effective on-site Coulomb repulsion (U_{eff}), they are in the proximity of the Mott insulating state. The ET superconductors having T_c more than 10K are such examples. We describe the overview of them with polymerized anions, emphasizing their curious phenomena in the normal and SC states, some of which are ascribable to the strongly correlated electrons.

A C₆₀ molecule is a weak electron acceptor which affords weak CT complexes with conventional TTF derivatives.² In order to generate carriers into them, the doping of alkali metals into a single crystals of a CT complex of C₆₀ under mild conditions were adopted.

DONOR PACKING, BAND STRUCTURES, MOTT CRITERION

In 10K class κ -(ET)₂X (X=polymerized anion),³ orthogonally aligned ET dimers form 2D conducting layer which is sandwiched between the polymerized anion layers (Fig. 1a). The HOMO bands are split into an upper- and a lower bands due to the dimerization (Fig. 1b). The HOMO band is assumed to be 3/4 filled (or upper HOMO band is 1/2 filled) provided that both the charge of the anion X is -1 and the U_{eff} is negligible compared to the band width of the upper HOMO band (W_U). The energy splitting of the upper- and the lower HOMO bands (ΔE) corresponds to the dimerization energy of a dimerized ET pair. The on-site Coulomb repulsion of a dimer is expressed as

$$U_{\text{dimer}} = \Delta E + [U_0 - (U_0 + 4\Delta E^2)^{1/2}]/2$$

where U_0 is an on-site Coulomb repulsion of a molecule. Since the U_0 of a ET molecule is much larger than the ΔE values of ET molecules, U_{dimer} is approximated as ΔE . So the Mott criterion is modified for the ET complexes which have dimerized donor pair as "if ΔE is sufficiently larger than the band width of the upper HOMO band ($\Delta E > W_U$), the electronic system will turn into a Mott-insulating state".

The ratio of the magnitudes of the ΔE and the W_U can distinguish whether the system is a Mott insulator or not. Actually, a plot of $\Delta E/W_U$ vs. W_U (Fig. 2) indicates that the κ -type salts of Cu(NCS)₂ (salt B, 9), Cu[N(CN)₂]Br (salt C, 8), Ag(CN)₂H₂O (7), and Cu(CN)[N(CN)]₂ (salt A, 6), which exhibit a semiconductive-like anomaly (7,8,9) or a hump (6) at higher temperatures, locate between the metallic ones (β -I₃(10), κ -I₃(11)) and Mott insulators (β '-IBrCl(1), β '-ICl₂(2), TCNQ complex (triclinic)(3) and κ -Cu₂(CN)₃(5). The metallic κ '-Cu₂(CN)₃(4) is

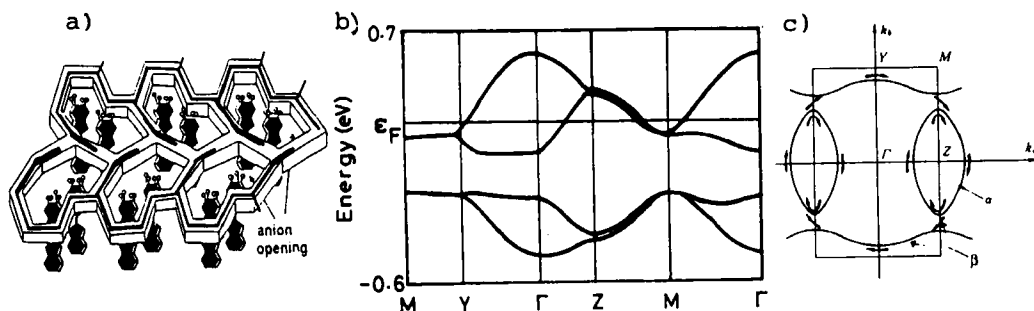


FIGURE 1 Schematic crystal structure(a), energy dispersion(b), and Fermi surface(c) of κ -(BEDT-TTF)₂(CN)[N(CN)₂].

converted from the Mott insulator $\kappa\text{-Cu}_2(\text{CN})_3$ by changing small amount (88-1200ppm) of Cu(+1) to Cu(+2).¹ So originally (4) should be a Mott insulator). The points for $\kappa\text{-Cu}[\text{N}(\text{CN})_2]\text{Cl}$ (salt D, 12) and $\kappa\text{-Cu}[\text{N}(\text{CN})_2]\text{Br}$ (8') in Fig. 2 are derived based on the crystal structures at 127K.⁴ Assuming that the change of the $W_U/\Delta E$ and the W_U values of the D salt from RT to 127K is the same magnitude as that of the C salt, the point of (12') is estimated for the RT values for the D salt, which locates in the proximity of the region of Mott insulator. Furthermore, if we include the effect of the anion, it is obvious that the less polarizable Cl ion is not advantageous to reduce the on-site Coulomb repulsion compared with Br, CN and SCN ions. That will make the $\text{Cu}[\text{N}(\text{CN})_2]\text{Cl}$ salt closer to the regime of Mott insulator.

Fig. 1c shows the calculated Fermi surface based on the crystal structure at RT.⁵ There is a gap between 1D electron-like Fermi surface and 2D cylindrical hole-like one (α -orbit, the ratio of the area of α -orbit (F_α) vs. that of the first Brillouin zone (F_B) is presented in Table 1) in the salts of $P2_1$ space group (A,B), while such gap does not exist in those of $Pnma$ space group (C,D). Several band parameters are summarized in Table 1.

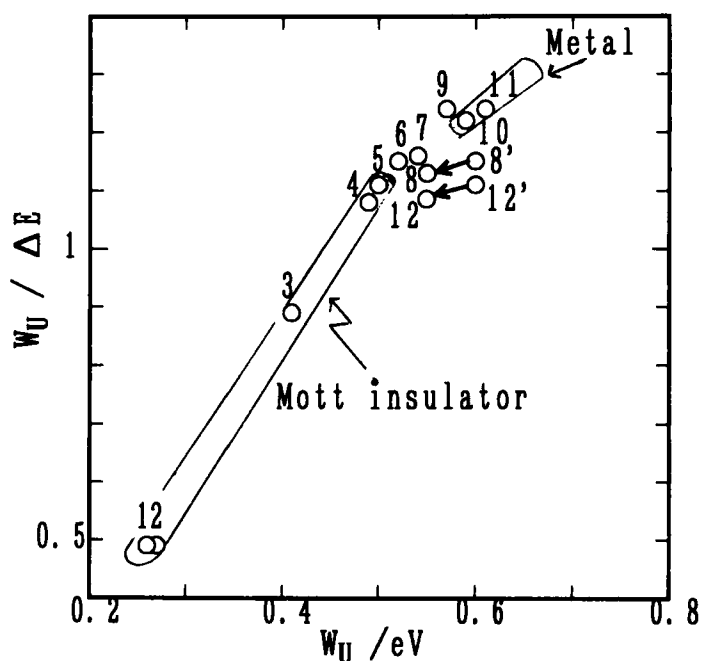


FIGURE 2 A plot of $\Delta E/W_U$ vs. W_U of $\kappa\text{-(BEDT-TTF)}_2\text{X}$

TABLE I Ligands, Tc of H and D-salts, Band parameters of 10K class SCs.

Salt	X'	Y'	Tc(K)		W (eV)	W _U (eV)	ΔE (eV)	D(ε _F) states/eV	F _α /F _B ·ET·spin (%)
			H & D						
			salt						
A	CN	N(CN) ₂	11.2	12.3(1 bar)	1.03	0.52	0.45	1.00	18
B	NCS	NCS	10.4	11.2(1 bar)	1.08	0.57	0.46	0.91	18
C	N(CN) ₂	Br	11.8	11.2(1 bar)	1.08	0.55	0.49	0.98	18
D*	N(CN) ₂	Cl	12.8	13.1(0.3kbar)	1.18	0.60	0.54	0.80	19

*The band parameters of the D salt is based on the structure at 127K.

ANION STRUCTURE

There are two kinds of ligands (X' and Y') in the anion polymer.³ The ligand X' bridges Cu(+1) ions to form a zig-zag infinite chain and the another ligand Y' coordinates to the Cu ion as a pendant. In the salt A, the N(CN)₂ ion is a pendant, while it works as the bridging part in the salts C and D. The anion chains of the salt C are reported to have weak 2D interactions due to weak atomic contacts between Y' in a chain and central N atom of the N(CN)₂ ligand in the neighboring chain.^{3c} On the other hand, the anion chains in other three salts are much separated and have 1D character. In order to keep the thermal contraction small, the use of a structurally 2D anion layer is effective, since the big thermal contraction of organic crystals is one of the depressing factor of Tc. Short atomic contacts are observed between the terminal ethylene groups of ET molecule and the anion atoms in the proximity of the anion opening. The conduction electrons are coherent and can behave as nearly free electrons within 2D conducting layer, while the electrons may transport by tunneling process through the anion opening. The pattern of the anion opening decides the donor packing motif^{5a} and both the anion thickness and the anion-donor interaction decide the interlayer coupling strength or the magnitude of 3D character. Thin anion layer composed of large anion unit is preferable to realize high Tc ET salts from the point of the dimensionality and the density of states.

ELECTRICAL CONDUCTIVITY, T_c , ISOTOPE EFFECT, REENTRANT SC

Though the band calculation, which excludes the electron correlation, indicates the similar Fermi surfaces among them, they show different conductivity behaviors (Fig. 3).³ The A salt shows monotonical decrease of resistivity with upper curvature (some hidden hump exists around 150K) down to the SC transition ($T_c=11.2$ K for the hydrogenated (H)-salt, 12.3K for the deuterated(D)-salt).^{3a} The B salt shows a prominent resistivity peak at 80-90K followed by a metallic behavior with $T_c=10.4$ K (H-salt) and 11.2K (D-salt).^{3b}

The H-salt of the C salt shows a similar behavior to that of the B salt, though the resistivity peak is at lower temperature (60-90K) than that of the B salt, below which it shows metallic behavior with $T_c=11.2$ K.^{3c} The D-salt of the C salt shows peculiar behaviors which are categorized into four groups (Fig. 3b).⁶ Curve [1] is the same temperature dependence as that of the H-salt and T_c of the samples of this behavior is the highest among the four groups. The T_c of the D-salt is a little (ca. 0.6K) lower than that of the H-salt. The shift of T_c by the isotope substitution is in the expected direction from the BCS theory (normal isotope shift). However, the C salt is the only one which shows the normal shift among the 10K class four salts (A-D). The other three (A,B,D) show inverse isotope shift if the molecular weight of the

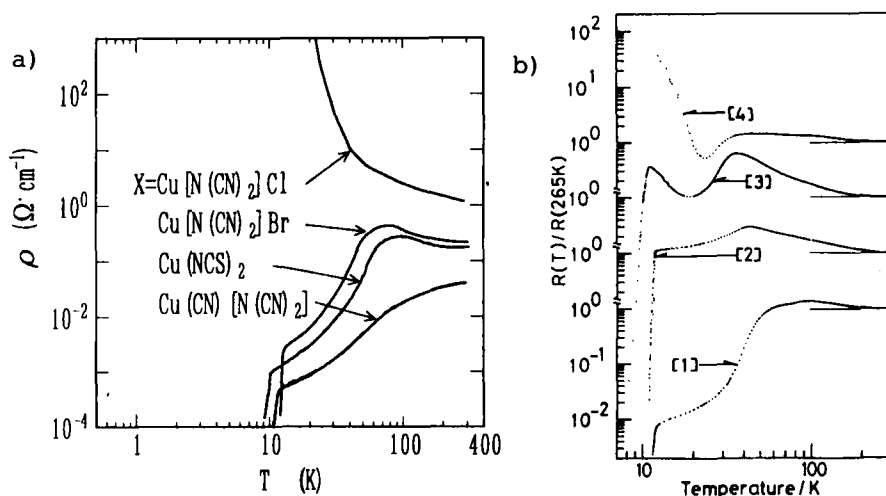


FIGURE 3 Temperature dependencies of resistance of $\kappa\text{-(BEDT-TTF)}_2\text{X}$; $\text{X}=\text{Cu}(\text{CN})[\text{N}(\text{CN})_2]$, $\text{Cu}(\text{NCS})_2$, $\text{Cu}[\text{N}(\text{CN})_2]\text{Br}$ and $\text{Cu}[\text{N}(\text{CN})_2]\text{Cl}$ (a) and four typical D-salts of the $\text{Cu}[\text{N}(\text{CN})_2]\text{Br}$ salt (b).

ET molecule is the isotope mass.⁷ One crystal (Curve [4]) shows a broad resistivity plateau between 90K and 40K followed by a narrow metallic region down to 24K, below which it shows a sharp resistivity increase instead of SC. In spite of these different behaviors in Fig. 3b, all the crystals of the D-salt have the lattice parameters in excellent agreement with those of the ordinal H-salt within experimental error.

The D salt exhibits rather similar temperature dependence of resistivity to Curve [4] in Fig.3b, though no trace of metallic behavior is seen above 22K. It shows a semiconductor($\epsilon_a=12\text{meV}$)-to-semiconductor($\epsilon_a=52\text{meV}$) transition at around 35-40K^{3d} and then a weak ferromagnetism is observed below 22K due to the antiferromagnetic(AF) spin canting in the 2D ET (ac) plane with the canting angle of ca. 0.1° .⁸ The easy axis is the b axis. A trace of SC appears in the weak ferromagnetic phase below 12K in the H-salt but not in the D-salt.⁹ The SC phase is stabilized by the application of weak pressure and it shows a similar temperature dependence of resistivity to those of the B and C salts in Fig.3 with $T_c=12.8\text{K}$ (H-salt) and 13.1K (D-salt) at 0.3kbar.^{7c}

One of the explanations of the semiconductive-like behavior at higher temperatures in the B and C salts is the strong electron correlation.¹⁰ It should be stressed here that there is a weak metallic region just above this fuzzy semiconductive region. This makes the understanding of the electronic structure of the fuzzy region very complicated. Since the spin susceptibility measurements¹¹ reveal that these two salts (H-salt of B,C) have similar magnitude and temperature dependence, which can be ascribable to Pauli paramagnetism, to those of the A and D salts above ca. 60K, these four salts are thought to have common electronic structure in this region (Fig.4).

The anisotropic temperature dependencies of the thermopower of the B and C salts in this region are quantitatively reproduced by using the calculated Fermi surfaces when the magnitude of the band dispersion is reduced. In the case of the Mott insulator, $\kappa\text{-Cu}_2(\text{CN})_3$ salt, its anisotropic thermopower cannot be reproduced at all from its calculated Fermi surface.¹ These results suggest that these salts have Fermi surfaces even at higher temperatures. Therefore, the electronic state in this region should not be either an intrinsic or Mott insulating state. However, it is not the conventional metallic state. Tentatively this state is named as fuzzy metal, which is very close to a Mott insulator.

The \underline{D} salt has a further complicated feature in the SC state. Below the SC phase appears a new non-metallic phase.⁹ For example under 380 bar well below the offset of SC at 12.1K, a sharp resistivity increase appears at 6.7K. This curious non-metallic phase is suppressed above 550 bar but reappears by the magnetic field cycling. The resistive ground state below SC state may be magnetic but is not understood yet.

The conductivity at RT, conductivity anisotropy $\sigma_{\parallel}/\sigma_{\perp}$, critical field (H_{c2}), GL coherent length (ξ) are summarized in Table 2. The smaller the conductivity anisotropy, the higher the 3D nature and the higher T_c is realized.

H_{c2} , MAGNETORESISTANCE, SHUBNIKOV-de HAAS AND OTHERS

Since the resistive transition by the magnetic field is broad, like oxide superconductors, due to either a flux-flow or distribution of T_c , the conventional determination of H_{c2} values by taking the midpoint of the resistive transition is not valid. However, at this stage there are no reliable methods to obtain intrinsic H_{c2} values (H_{c2} values in Table 2 are the conventional ones and thus tentative). Also the conventional

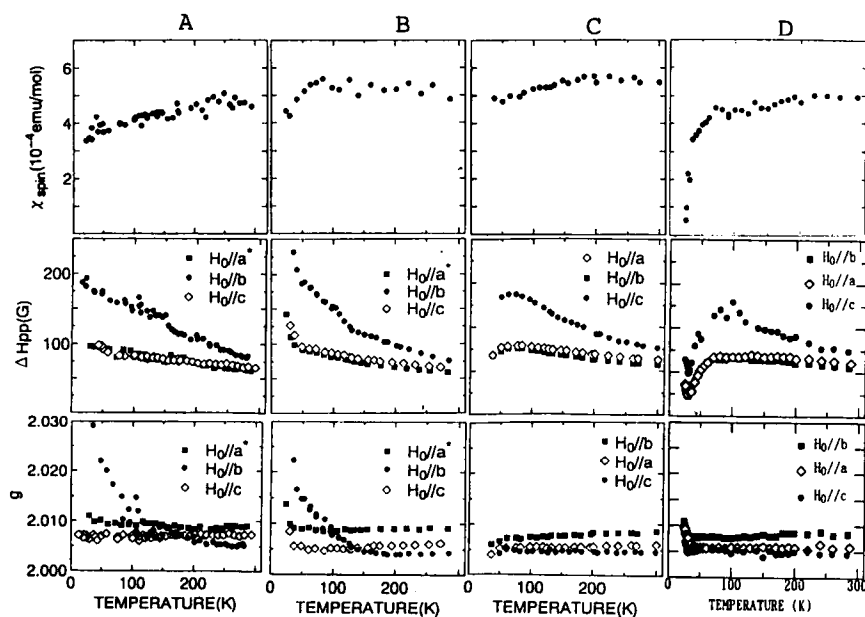


FIGURE 4 Temperature dependencies of the ESR parameters of κ -(BEDT-TTF) $_2$ X; X=Cu(CN)[N(CN) $_2$](A), Cu(NCS) $_2$ (B), Cu[N(CN) $_2$]Br(C) and Cu[N(CN) $_2$]Cl(D).

TABLE II Several physical properties of 10K class SCs.

salt	σ_{RT}	$\sigma_{\parallel}/\sigma_{\perp}$	$H_{c2}(0)$		ξ (Å)		SdH (or dHvA)		ADMRO
	Scm^{-1}		$\parallel 2D$	$\perp 2D$	\parallel	\perp	α (T)	β (T)	
<u>A</u>	50	230	21.5	6.8			no	no	no
<u>B</u>	40	600	24.5	5.5	29	3.1	600-666	3890	yes
<u>C</u>	48	200	30.6	7.4	23	5.8	156	no	no
<u>D</u>	2	100					609	3991	yes

analysis to obtain GL coherence length(ξ) is thus not adequate, and ξ values obtained by the renormalization theory are presented in Table 2. These values show strong 2D character of these salts. Especially it is noteworthy that the ξ_{\perp} values are shorter than the corresponding lattice constants.

The Shubnikov-de Haas (SdH), de Haas-van Alphen (dHvA) and angle dependent magnetoresistance oscillations (ADMRO) are powerful tools to investigate the Fermi surfaces of metals topologically. The results of these oscillations at present stage is summarized in Table 2. The B salt shows SdH effects (600-666T) corresponding to the extremal cross-sectional area of 16-18% of the first B_z in excellent agreement with the calculated α -orbit.^{5b} The cyclotron mass $m_c=3.5-3.6m_e$ of the α -orbit is considerably larger than the calculated band mass $m_b=0.9m_e$ and the cyclotron resonance mass $m_{cr}=1.18m_e$ indicating a strong electron correlation in this salt. The magnetic breakdown oscillations (3890T) were observed above 20T with a large electron trajectory (β -orbit, 100% of the first B_z , $m_c=6.5-7m_e$). At ambient pressure no SdH effects were observed in the C salt. At ca. 9kbar, oscillations of 156T which correspond to ca. 4.4% of the first B_z ($m_c=0.95m_e$) were detected.¹² This does not agree with the calculated Fermi surface. Furthermore, no oscillations corresponding to the β -orbit were observed. These facts suggest the occurrence of some structural modification at low temperatures. The D salt exhibits SdH effects under pressure and above 10T.¹³ The lower frequency (609T at 7.7kbar) corresponds to the α -orbit and the higher one (3991T at 7.7kbar) to β -orbit. The ADMRO results indicate that the orthorhombic symmetry is lowered, resulting in the

appearance of the energy gap between the 1D and 2D like Fermi surfaces. Any quantum oscillations have been detected on the A salt so far.

The $1/T_1T$ values derived from the ^{13}C NMR measurements of the B, C, D salts showed the same temperature dependence down to 60K among them,¹⁴ in agreement with the ESR results. They increase steadily to the twice that of the RT value at 60K. This enhancement is interpreted by the growth of the short range order of the AF fluctuation. Below 60K, they behave differently. The D salt has a divergent peak at 26-27K due to the growth of the AF ordering. On the other hand, the growth of the AF fluctuation is somehow suppressed in the B and C salts, and they show peaks in $1/T_1T$ at around 50K then decrease.

These four salts exhibit basically the similar temperature dependence of ESR properties (Fig. 4)¹¹ above 150K. The χ_{spin} values at RT ($4\text{--}6 \times 10^{-4}$ emu/mol) are expected magnitude for the Pauli paramagnetism with strong electron correlation. In the case of a Mott insulator, $\kappa\text{-Cu}_2(\text{CN})_3$ salt, the χ_{spin} is ca. 8×10^{-4} emu/mol. While in the case of the conventional metal $\beta\text{-I}_3$, $\chi_{\text{spin}} = 4.6 \times 10^{-4}$ emu/mol at RT. The χ_{spin} values decrease gradually down to 20K for the salts of A, B and C. For the D salt, they decrease rapidly below 35K because of the occurrence of AF fluctuation. The temperature dependencies of the line width ΔH and the g -values are categorized into two groups depending on the space group of the crystal. In the case of Pnma (C salt) or $P2_1/c$ (ex. $\kappa'\text{-Cu}_2(\text{CN})_3$ salt), in which there are no gap between the 1D and 2D Fermi surfaces, the ΔH values show broadening down to ca. 60K then sharpening. That is consistent with the $1/T_1T$ results by ^{13}C NMR. The g -values are constant down to ca. 60K then decrease. In the case of $P2_1$ group (A, B salts), the ΔH and the g -values show extensive broadening below 35K. Especially these values along the b -axis start to show pronounced broadening even at 150K. This anisotropic broadening in ΔH and g -values may suggest the nesting character of the 1D Fermi surface, but it is not consistent with both the ^{13}C NMR results and the resistivity results which do not show any traces of instability at lower temperatures.

SUMMARY (PROBLEMS TO BE SOLVED IN 10K CLASS SCs)

There are so many factors which are connected with the curious structural and physical properties of molecular conductors, namely the

softness of molecule and crystal due to high polarizability, high compressibility against the pressure and heat, a variety of molecular vibrations and conformations, weak cohesive interactions, low dimensionality, big molecular size, etc. The 10K class ET SCs discussed here have additional aspects that they are in the proximity of Mott insulators ($\Delta E \approx W_U$) which induce further curiosity in the physical properties. The followings are the some problems to be understood:

1. What causes the semiconducting-like behavior or what is the electronic structure in the fuzzy metallic region? 2. What causes the extensive increase of ΔH and g -values at low temperatures in only $P2_1$ space group salts and why anisotropically? And what theory can be applied, instead of the Elliott mechanism, for the ΔH and g -values of the organic metals? What kinds of magnetic instability are involved in the A, B, C salts above SC state? 3. The extended Huckel band calculation is successful to some extent. However, why the magnitude of transfer interactions should be reduced by ca. 1/5 to reproduce the temperature dependence of thermopower? 4. Why some but not all of organic SCs show large inverse isotope effect on T_c ? 5. Why the D salt shows reentrant SC and what is the nature of the non-metallic ground state? 6. What is the low-temperature structures of the C and D salts which gave the SdH effects different from those estimated from the RT crystal structures? And why the A salt does not show oscillations? And generally, 7. are there gap or not in SC? Is the Cooper pair singlet or triplet? What is the mechanism of organic SCs?

SUPERCONDUCTIVITY OF C_{60} -CT COMPLEXES

Since the C_{60} molecule is a weak electron acceptor, it gives neutral CT complexes with a number of electron donors including TTF analogues such as OMTTF, BEDT-TTF, BEDO-TTF, EDT-TTF, etc. Therefore, the single crystal of OMTTF· C_{60} ·benzene is an insulator of 10^{-8} Scm^{-1} at RT. The injection of carrier was performed by the doping of alkali metals. In order to have a single crystal-to-single crystal transformation and to avoid the decomposition of the pristine CT complex, the doping was done at lower temperatures (50–55°C for K and 64–67°C for Rb for more than 10 days) than the decomposition temperature of the crystal (>150°C). The superconductivity was examined by low field microwave absorption (LFMA)

and SQUID magnetization measurements.

The temperature dependence of magnetization¹⁵ and LFMA (Fig. 5) of K doped and Rb doped OMTTF·C₆₀·benzene show that the K doped material has T_c of ca.17-18.8K with anomalous structures at ca. 12 and 8K, while LFMA indicates SC starts below 18.5K and also some anomaly below 14K. In the case of Rb doping, the magnetization shows T_c=23-26K with anomalies at ca.12 and 8K and the LFMA indicates SC starts below 26.7K. The crystal structure analysis and the EPMA/SEM studies of the K doped crystal show that the doping level is low (ca. 0.6 K per complex by lattice expansion and K:complex=x:1 with x≤1.8 by EPMA/SEM). It was found that the superconducting phase is not K₃C₆₀, though T_c's of which is close to the one we observed. The doping did not change much the 2D array of C₆₀ molecules in the pristine crystal. Although the position of the doped K is not determined yet, the doped crystal will show 2D character in its superconductivity.

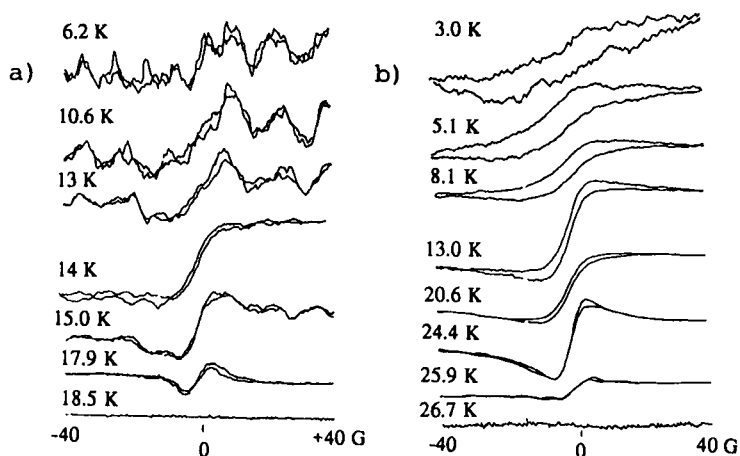


FIGURE 5 Temperature dependence of the LFMA signals of K (a) and Rb (b) doped OMTTF·C₆₀·benzene

REFERENCES

1. T. Komatsu, N. Matsukawa, T. Inoue, G. Saito, J. Phys. Soc. Jpn., in press
2. G. Saito, T. Teramoto, A. Otsuka, Y. Sugita, T. Ban, M. Kusunoki, K. Sakaguchi, Synth. Metals, 64, 359(1994)
3. a) A salt: T. Komatsu, T. Nakamura, N. Matsukawa, H. Yamochi, G. Saito, H. Ito, T. Ishiguro, M. Kusunoki, K. Sakaguchi, Solid State Commun., 80, 843(1991); b) B salt: H. Urayama, H. Yamochi, G. Saito, K. Nozawa, T. Sugano, M. Kinoshita, S. Sato,

- K.Oshima, H.Kawamoto, J.Tanaka, *Chem.Lett.*, 1988, 55; c) C salt: A.M.Kini, U. Geiser, H.H.Wang, K.D.Carlson, J.M.Williams, W.K.Kwok, K.G.Vandervoort, J.E. Thompson, D.L.Syupka, D.Jung, M.H.-Wangbo, *Inorg.Chem.*, 29(1990)2555; d) D salt: J.M.Williams, A.M.Kini, H.H.Wang, K.D.Carlson, U.Geiser, L.K.Montgomery, G.J.Pyrka, D.M.Watkins, J.M.Kommers, S.J.Boryschuk, A.V.S.Crouch, W.K.Kwok, J.E.Schirber, D.L.Overmyer, D.Jung, M.-H.Wangbo, *Inorg.Chem.*, 29(1990)3272
4. U.Geiser, A.J.Shultz, H.H.Wang, D.M.Watkins, D.L.Stupka, J.M.Williams, J.E. Schirber, D.L.Overmyer, D.Jung, J.J.Novoa, M.-H.Whangbo, *PhysicaC*174, 475(1991)
5. a) A salt: H.Yamochi, T.Komatsu, N.Matsukawa, G.Saito, T.Mori, M.Kusunoki, K.Sakaguchi, *J.Am.Chem.Soc.*, 115(1993)11319; b) B salt: K.Oshima, T.Mori, H.Inokuchi, H.Urayama, H.Yamochi, G.Saito, *Phys.Rev.B*38, 938(1988); C salt: ref.3c, D salt: ref.3d
6. T.Komatsu, N.Matsukawa, T.Nakamura, H.Yamochi, G.Saito, H.Ito, T.Ishiguro, *Phos.Sulfur, Silicon*, 67, 295(1992)
7. a) A salt: G.Saito, H.Yamochi, T.Nakamura, T.Komatsu, N.Matsukawa, T.Inoue, H.Ito, T.Ishiguro, M.Kusunoki, K.Sakaguchi, *Synth.Met.*, 55- 57, 2883(1993); b) B salt: G.Saito, H.Urayama, H.Yamochi, K.Oshima, *Synth.Metals*, 27, 331 (1988); c) D salt: J.E.Schirber, D.L.Overmyer, K.D.Carlson, J.M.Williams, A.M.Kini, H.H.Wang, H.A.Charlier, B.J.Love, D.M.Watkins, G.A.Yaconi, *Phys.Rev.B*44, 4666(1991)
8. U.Welp, F.Fleshler, W.K.Kwok, G.W.Crabtree, K.D.Carlson, H.H.Wang, U.Geiser, J.M.Williams, V.M.Hitsman, *Phys.Rev.Lett.*, 69, 840(1992)
9. Y.V.Sushko, H.Ito, T.Ishiguro, S.Horiuchi, G.Saito, *Solid State Commun.*, 87, 997(1993), *J.Phys.Soc.Jpn.*, 62, 3372(1993)
10. a) L.I.Buravov, A.V.Zvarykina, N.D.Kushch, V.N.Laukhin, V.A.Merzhanov, A.G. Khomenko, E.B.Yagubskii, *Sov.Phys.JETP*, 68, 182(1989); b) N.Toyota, T. Sasaki, *Solid State Commun.*, 74, 361(1990)
11. a) T.Nakamura, T.Nobutoki, T.Takahashi, G.Saito, H.Mori, T.Mori, *J.Phys.Soc.Jpn.*, 62(1993)4373, b) M.Kubota, G.Saito, H.Ito, T.Ishiguro, N.Kojima, this proceedings
12. M.V.Kartsovnik, G.Yu.Logvenov, H.Ito, T.Ishiguro, G.Saito, *Phys.Rev.B*52, in press
13. Y.Yamauchi, M.V.Kartsovnik, T.Ishiguro, M.Kubota, G.Saito, *J.Phys.Soc.Jpn.*, in press
14. K.Kanoda *et al.*, private communication
15. A.Otsuka *et al.*, this proceedings